JOURNAL OF GUIDANCE, CONTROL, AND DYNAMICS
Vol. 20, No. 2, March–April 1997

Near-Optimal Guidance Law for Ballistic Missile Interception

John J. Dougherty*
TRW Systems Integration Group, San Bernardino, California 92402
and
Jason L. Speyer†
University of California, Los Angeles, Los Angeles, California 90095

A perturbation procedure is applied to the problem of finding an optimal control for a ballistic missile interceptor. Certain forces, such as thrust and gravity, are assumed to dominate the equations of motion. The optimal control problem is integrable if the remaining forces are neglected; the approximate effects of the neglected forces can be calculated noniteratively and added to the solution. For certain trajectories, however, the aerodynamic forces are not negligible. Including the aerodynamics directly in the dominant dynamics destroys the analytical solution upon which the procedure depends. Instead, approximations of the aerodynamic forces are included through narrow pulse functions. This technique produces a good approximation to the optimal control and is computationally more efficient than previous methods. Provisions also are made to account for the interceptor's coast phase and terminal constraints. The near-optimal guidance law is used to produce intercept trajectories against a number of target trajectories. The approximate trajectories compare well with numerically generated optimal trajectories.

I. Introduction

THE necessary conditions for the optimal control of a ballistic missile interceptor form a nonlinear two-point boundary value problem. Direct numerical solutions of this problem require iteratively integrating nonlinear differential equations. Not only does this involve substantial computation, but the convergence properties can be poor. Often, solving the two-point boundary value problem in real time is not feasible. When a real-time controller is required, another approach is necessary.

A technique that has been shown to produce good approximations to the optimal control for a variety of problems uses a perturbation procedure.[1,2] Some forces are assumed to dominate the equations of motion; the equations are such that the optimal control problem is integrable if the remaining forces are neglected. Once this underlying problem is solved, the approximate effects of the neglected forces can be calculated without iteration. The chief advantage of this approach is that it involves only the solution of a set of coupled nonlinear equations and the noniterative integration of quadratures. It is therefore feasible to host the algorithm in onboard flight computers and perform the optimization in real time.

Feeley[3,4] used a perturbation approach for obtaining an approximate optimal control for a two-stage boost vehicle that was powered throughout flight. He noted that the thrust and gravity forces dominate the aerodynamic forces and that the zeroth-order differential equations, including only the dominant forces, have an analytical solution. Mishne and Speyer[5] and Speyer and Crues[6] applied this approach to the problem of an aeroassisted plane-change maneuver. The approximation used in those works is valid when the aerodynamic forces dominate gravitational forces. Ilgen et al.[7] solved a version of the problem using a calculus-of-variations approach rather than a dynamic programming approach. Calise and Melamed[8–10] considered the initial and terminal portions of an aeroassisted plane change, where aerodynamic forces are still small, in addition to the aerodynamically dominated region. They used matched asymptotic expansions to derive a uniformly valid solution.

The perturbation approach also can be applied to the problem of generating near-optimal trajectories for a vehicle designed to intercept medium range ballistic missiles. The interceptor has several boost stages and a long unpowered coast phase. Although the problem is similar to the one solved by Feeley,[3,4] extensions to his work have been made to accommodate the multiple stages and the differing boundary conditions. Furthermore, the assumption that gravity dominates aerodynamics during the coast phase necessitates special treatment of the zeroth-order constraints. The extensions to Feeley's work and the treatment of the constraints are discussed in Secs. II and III.

Most significantly, the assumption that aerodynamic forces are only a perturbing effect is not valid for longer trajectories. Including the aerodynamics directly in the dominant dynamics would destroy the analytical solution to the zeroth-order differential equations. Instead, approximations of the aerodynamics can be included in the dominant dynamics in such a way that the analytical zeroth-order solution is preserved. Techniques for both the thrust and coast phases are considered. The technique used in the thrust phases is described in Sec. IV. This technique assumes a discontinuous form for the states and costates. The major effects of the aerodynamics are included in both the states and the costates without increasing the dimension of the zeroth-order problem. It is superior in this respect to previous approaches,[3,4,11] as described in Sec. VI. Another technique is possible for coast phases, as described in Sec. V.

The near-optimal guidance law was used to generate intercept trajectories against a number of target trajectories. Comparisons were made to optimal trajectories produced by a numerical solution to the full necessary conditions. Results and conclusions are provided in Secs. VII and VIII.

II. Basic Near-Optimal Solution

The two-dimensional equations of motion for the ballistic missile interceptor, in Cartesian coordinates, are

$$\frac{\mathrm{d}X_1}{\mathrm{d}t} = w_1 \tag{1}$$

$$\frac{\mathrm{d}X_3}{\mathrm{d}t} = w_3 \tag{2}$$

$$\frac{\mathrm{d}w_1}{\mathrm{d}t} = \frac{T_{\text{net}}}{m}\cos\Gamma - g_t\frac{X_1}{\sqrt{X_1^2+X_3^2}} - \frac{\rho V^2 S}{2m}\left(C_D\frac{w_1}{V} + C_L\frac{w_3}{V}\right) \tag{3}$$

$$\frac{\mathrm{d}w_3}{\mathrm{d}t} = \frac{T_{\text{net}}}{m}\sin\Gamma - g_t\frac{X_3}{\sqrt{X_1^2+X_3^2}} - \frac{\rho V^2 S}{2m}\left(C_D\frac{w_3}{V} - C_L\frac{w_1}{V}\right) \tag{4}$$

Received Jan. 19, 1996; revision received Oct. 21, 1996; accepted for publication Oct. 26, 1996.

*Staff Engineer, Strategic Systems Division. Member AIAA. E-mail: john.dougherty@trw.com.
†Professor, Department of Mechanical and Aerospace Engineering. Fellow AIAA. E-mail: speyer@seas.ucla.edu.

where T_{net} is the net thrust, m is the interceptor mass, Γ is the control, g_t is the gravity, ρ is the air density, V is the velocity magnitude, S is the interceptor aerodynamic reference area, and C_L and C_D are the lift and drag coefficients.[12] The coordinate frame is Earth-centered, with X_3 along the launch-site vertical and X_1 in the downrange direction.

The optimization problem is to minimize

$$J = \phi[\boldsymbol{x}(t_f), t_f] \tag{5}$$

subject to the dynamics (1–4), the constraints

$$\psi[\boldsymbol{x}(t_f), t_f] = 0 \tag{6}$$

and $\boldsymbol{x}(t_o)$ given. For the ballistic missile interceptor, the problem is to intercept a moving target (match terminal positions) in minimum time. The target is modeled as moving along a known ballistic path.

By making assumptions about the relative sizes of terms in Eqs. (3) and (4), the equations of motion are rewritten as

$$\frac{\mathrm{d}\boldsymbol{x}}{\mathrm{d}t} = \boldsymbol{f}(\boldsymbol{x}, \boldsymbol{u}) + \epsilon \boldsymbol{g}(\boldsymbol{x}, \boldsymbol{u}) \tag{7}$$

where $\boldsymbol{x} = [X_1 \;\; X_3 \;\; w_1 \;\; w_3]^T$ and $\boldsymbol{u} = \Gamma$. The primary dynamics $\boldsymbol{f}$ are assumed to dominate the secondary or perturbing dynamics $\boldsymbol{g}$. Specifically, if the thrust and most of the gravity can be assumed to dominate the aerodynamics and remaining gravity, Eqs. (3) and (4) can be rewritten as

$$\frac{\mathrm{d}w_1}{\mathrm{d}t} = \frac{T}{m}\cos\Gamma + \epsilon\frac{r_s}{H_\rho}\left[\frac{-pA_e}{m}\cos\Gamma - g_t\frac{X_1}{\sqrt{X_1^2 + X_3^2}} - \frac{\rho V^2 S}{2m}\left(C_D\frac{w_1}{V} + C_L\frac{w_3}{V}\right)\right] \tag{8}$$

$$\frac{\mathrm{d}w_3}{\mathrm{d}t} = \frac{T}{m}\sin\Gamma - g_s + \epsilon\frac{r_s}{H_\rho}\left[\frac{-pA_e}{m}\sin\Gamma + g_s - g_t\frac{X_3}{\sqrt{X_1^2 + X_3^2}} - \frac{\rho V^2 S}{2m}\left(C_D\frac{w_3}{V} - C_L\frac{w_1}{V}\right)\right] \tag{9}$$

where g_s is the constant X_3 gravity component, T is the vacuum thrust, p is the atmospheric pressure, and A_e is the nozzle exit plane area. The thrust time history is assumed to be given (no throttle). The small parameter ϵ is the ratio of the atmospheric scale height H_ρ to the radius of the Earth r_s and is introduced for bookkeeping.

Unfortunately, the assumption that the aerodynamics are dominated by other forces is too strong for some problems. As described in Sec. IV, it is possible to include a large portion of the aerodynamic forces in the primary dynamics, but it must be done carefully, lest the computational advantages of the perturbation approach be lost. In essence, the division of forces assumed in Eqs. (8) and (9) is retained everywhere except at a finite number of points along the trajectory. For now, a description of the approach will be made with reference to Eq. (7) in general.

The necessary conditions for an optimal control are Eqs. (6) and (7) along with

$$H = \boldsymbol{\lambda}^T[\boldsymbol{f}(\boldsymbol{x}, \boldsymbol{u}) + \epsilon \boldsymbol{g}(\boldsymbol{x}, \boldsymbol{u})] \tag{10}$$

$$H_u = 0 \tag{11}$$

$$H_{uu} \geq 0 \tag{12}$$

$$\frac{\mathrm{d}\boldsymbol{\lambda}}{\mathrm{d}t} = -H_x^T \tag{13}$$

$$\boldsymbol{\lambda}(t_f) = \left(\frac{\partial\phi}{\partial\boldsymbol{x}} + \boldsymbol{\nu}^T\frac{\partial\psi}{\partial\boldsymbol{x}}\right)^T \tag{14}$$

$$H(t_f) + \frac{\partial\phi}{\partial t_f} + \boldsymbol{\nu}^T\frac{\partial\psi}{\partial t_f} = 0 \tag{15}$$

and the initial state equal to $\boldsymbol{x}(t_o)$, where $\boldsymbol{\lambda}$ is the costate vector and $\boldsymbol{\nu}$ is the Lagrange multiplier vector for the final constraints. These equations form a nonlinear two-point boundary value problem.

The approximate solution of the optimization problem proceeds as follows. The states, costates, constraint Lagrange multipliers, control, and final time are expanded about the small parameter ϵ; for instance,

$$\boldsymbol{x}(t) = \boldsymbol{x}_0(t) + \epsilon\boldsymbol{x}_1(t) + \epsilon^2\boldsymbol{x}_2(t) + \cdots \tag{16}$$

By expanding the Euler–Lagrange equations in Taylor series about the zeroth-order quantities, substituting the expansions for the states, costates, etc., and grouping by powers in ϵ, sets of necessary conditions for each order in ϵ are obtained. If the necessary conditions to zeroth order are of a form allowing analytical integration of the differential equations, then solution of the zeroth-order problem becomes a matter of finding roots to a nonlinear system of equations. The solution to higher order can be obtained by quadrature integrals; the required functions are given by transition functions obtained from the zeroth-order problem.[3–7,12] The control at the current time t_0 is calculated from the zeroth- and higher-order terms as

$$\boldsymbol{u}(t_0) = \arg\min_{\underline{u}}[\boldsymbol{\lambda}_0(t_0) + \epsilon\boldsymbol{\lambda}_1(t_0)]^T\left[\boldsymbol{f}\left(\boldsymbol{x}_{t_0}, \underline{u}\right) + \epsilon\boldsymbol{g}(\boldsymbol{x}_{t_0}, \underline{u})\right] \tag{17}$$

Note that a chief advantage of this approach is that it allows for the easy inclusion of highly nonlinear forces in the perturbing dynamics.

To integrate the zeroth-order differential equations obtained from Eqs. (1), (2), (8), (9), and (13), they are rewritten in terms of a new independent variable m, the vehicle mass, where $\mathrm{d}m/\mathrm{d}t = -\sigma T$. The differential equations then give rise to a quadratic polynomial in m under a radical in the denominator of an integral. It can be shown that the discriminant of the quadratic polynomial is a constant of the motion.[13]

Feeley[3,4] provided an analytical solution to these zeroth-order differential equations for the case of constrained final velocity. For the ballistic missile interceptor problem, however, the final velocity is unconstrained and Feeley's solution must be modified[13]; the appropriate integrals are obtained from standard tables.[14]

III. Treatment of Constraints

The approximate solution of the optimal control problem is contingent on the existence of a zeroth-order solution. Under some circumstances, a zeroth-order solution may not exist, even though the full optimal control problem has a solution. Consider a situation where the primary forces are not affected by the control:

$$\dot{\boldsymbol{x}} = \boldsymbol{f}(\boldsymbol{x}) + \epsilon\boldsymbol{g}(\boldsymbol{x}, \boldsymbol{u}) \tag{18}$$

This can happen when, for example, the dominant term in the dynamics is gravity, and the aerodynamics, including the control, are assumed to be perturbing forces.[7,15] For the problem of an interceptor with a coast phase following boost, the control vanishes from the primary dynamics at thrust termination. After thrust termination, the zeroth-order trajectory is fixed, the zeroth-order boundary conditions cannot be met in general, and the zeroth-order problem has no solution.

A similar situation can occur prior to thrust termination. An $\boldsymbol{x}(t_o)$ for which there is a full-dynamics optimal trajectory includes the optimal thrust termination state $\boldsymbol{x}(t_t)$. A zeroth-order trajectory initialized from $\boldsymbol{x}(t_t)$ will not meet the terminal constraints. Let $\boldsymbol{x}_0(t_t)$ be a state for which a zeroth-order trajectory will meet the terminal constraints; note that $\boldsymbol{x}_0(t_t) \neq \boldsymbol{x}(t_t)$. For $t_t - t_o$ sufficiently small, there is no control that can drive the zeroth-order trajectory from $\boldsymbol{x}(t_o)$ to $\boldsymbol{x}_0(t_t)$ and thus no zeroth-order solution. Furthermore, if $t_t - t_o$ is just large enough to allow a zeroth-order control producing $\boldsymbol{x}_0(t_t)$, this control will be very large and very different from the optimal control, because the assumption that the thrust dominates the aerodynamics is flawed. The resulting zeroth-order plus first-order approximation to the optimal control likely will be poor.

The approach used here to obtain a suitable zeroth-order trajectory transforms some of the terminal constraints to linear penalty functions using previously computed Lagrange multipliers.[16] The zeroth-order solution to the resulting problem forms a good approximation to the optimal control, but with first-order errors in the penalized constraints. When the first-order corrections are added, however, the control satisfies the original set of terminal constraints. In this way, a controllability problem is effectively avoided.

IV. Including Aerodynamics in the Primary Dynamics

The zeroth-order equations of motion (8) and (9) presented in Sec. II do not include any aerodynamic forces. For some trajectories, this is a good approximation. The inclusion of aerodynamic forces through the first-order correction is effective. For other trajectories, particularly longer-range trajectories with long coasts, the aerodynamic forces have a large effect on the shape of the trajectory, and it is necessary to include at least some of them in the zeroth-order solution. The chief difficulty here is that the analytical solutions to the zeroth-order problem are very fragile; the addition of state- or control-dependent dynamics tends to render the problem unsolvable analytically. The problem, then, is to write the equations of motion in the form of primary and perturbing forces in such a way as to allow for analytical integration of the resulting zeroth-order differential equations.

A new technique examined here is to assume a discontinuous form for the states and costates. In a finite number of intervals between discontinuities, Eq. (7) and, in particular, Eqs. (8) and (9) are assumed to hold. At the discontinuities, the states are written, in expanded form, as

$$x_0\left(t_j^+\right) = x_0\left(t_j^-\right) + \mathcal{P}_j\left[x_0\left(t_j^-\right), u_0(t_j)\right] \tag{19}$$

$$\begin{aligned} x_1\left(t_j^+\right) &= x_1\left(t_j^-\right) + \mathcal{P}_{jx}\left[x_0\left(t_j^-\right), u_0(t_j)\right]x_1\left(t_j^-\right) \\ &\quad + \mathcal{P}_{ju}\left[x_0\left(t_j^-\right), u_0(t_j)\right]u_1(t_j) + k\mathcal{P}_j\left[x_0\left(t_j^-\right), u_0(t_j)\right] \end{aligned} \tag{20}$$

where

$$\mathcal{P}_j(x, u) = (t_{j+1} - t_j)\,(1/k)\,g(x, u) \tag{21}$$

and where $k = 1/\epsilon$. The superscripts $-$ and $+$ indicate the left- and right-hand limits of x_0 at t_j, and x and u as subscripts indicate partial differentiation. Between discontinuities, then, the aerodynamic forces are neglected and the analytical integrals discussed in the previous sections are applicable. The approximate effects of the aerodynamics are included in the zeroth-order problem at the discontinuity points, in what amounts to a coarse numerical integration. The error obtained by using a relatively few discontinuity points (integration steps) is quite tolerable, however, because the overall approximation can be greatly refined by solution of the corresponding higher-order problems. The number of discontinuity points is chosen to incorporate the bulk of the effects of aerodynamics in the zeroth-order problem; in practice, only a few points are necessary (less that five). Increasing the number of discontinuity points does produce a better zeroth-order approximation, but at the cost of more calculations.

The motivation for the form of Eqs. (19) and (20) can be seen as follows. Conceptually, the discontinuous solution corresponds to dynamics written in the form

$$\begin{aligned} \frac{\mathrm{d}x}{\mathrm{d}t} &= f(x, u) + \sum_{j=1}^{N} \mathcal{P}_j(x, u)\delta(t - t_{j+1}) \\ &\quad + \epsilon\left[g(x, u) - k\sum_{j=1}^{N}\mathcal{P}_j(x, u)\,\delta(t - t_{j+1})\right] \end{aligned} \tag{22}$$

where the presence of N discontinuities is indicated. When expansions for the states and control are substituted into Eq. (22), the dynamics are of the form

$$\frac{\mathrm{d}x_0}{\mathrm{d}t} = f(x_0, u_0) + \sum_{j=1}^{N}\mathcal{P}_j(x_0, u_0)\delta(t - t_{j+1}) \tag{23}$$

$$\begin{aligned} \frac{\mathrm{d}x_1}{\mathrm{d}t} &= f_x(x_0, u_0)x_1 + f_u(x_0, u_0)u_1 \\ &\quad + \sum_{j=1}^{N}\mathcal{P}_{jx}(x_0, u_0)\delta(t - t_{j+1})x_1 + \sum_{j=1}^{N}\mathcal{P}_{ju}(x_0, u_0)\delta(t - t_{j+1})u_1 \\ &\quad + g(x_0, u_0) + k\sum_{j=1}^{N}\mathcal{P}_j(x_0, u_0)\delta(t - t_{j+1}) \end{aligned} \tag{24}$$

$$\vdots$$

which motivate Eqs. (19) and (20). The function δ is a very narrow rectangle function with unit area and can be thought of as a Dirac delta function if an appropriate definition of the differential equation is made. The time t_{j+1} is the time at the end of stage j.

The corresponding differential equation for the costates is

$$\begin{aligned} \frac{\mathrm{d}\lambda}{\mathrm{d}t} &= -f_x^T(x, u)\lambda - \sum_{j=1}^{N}\mathcal{P}_{jx}^T(x, u)\lambda\delta(t - t_{j+1}) \\ &\quad + \epsilon\left[-g_x^T(x, u)\lambda + \frac{r_s}{H_\rho}\sum_{j=1}^{N}\mathcal{P}_{jx}^T(x, u)\lambda\delta(t - t_{j+1})\right] \end{aligned} \tag{25}$$

The analogs to Eqs. (23) and (24) can be obtained by expanding the quantities in Eq. (25) in powers of ϵ.

An expression for the values of the costates across the discontinuity is derived as follows. The differential of the cost function (5) augmented by the constraints can be written as

$$\begin{aligned} \mathrm{d}\bar{J} &= \left[\frac{\partial\Phi}{\partial t}\mathrm{d}t_f + \frac{\partial\Phi}{\partial x}\mathrm{d}x\right]_{t=t_f} \\ &\quad + \int_{t_o}^{t_j^-}\left[\left(\lambda^T\frac{\partial f}{\partial x} + \dot{\lambda}^T\right)\delta x + \lambda^T\frac{\partial f}{\partial u}\delta u\right]\mathrm{d}t \\ &\quad + \int_{t_j^+}^{t_f}\left[\left(\lambda^T\frac{\partial f}{\partial x} + \dot{\lambda}^T\right)\delta x + \lambda^T\frac{\partial f}{\partial u}\delta u\right]\mathrm{d}t \\ &\quad - [\lambda^T\delta x]_{t_o}^{t_j^-} - [\lambda^T\delta x]_{t_j^+}^{t_f} \end{aligned} \tag{26}$$

where the integral has been broken around the discontinuity at t_j and where the symbol δ here and following indicates a variation. Following the usual procedure,[17] a necessary condition for an optimal control is obtained from Eq. (26) as

$$-\lambda^T\left(t_j^-\right)\delta x\left(t_j^-\right) + \lambda^T\left(t_j^+\right)\delta x\left(t_j^+\right) = 0 \tag{27}$$

Now, by taking the variation of Eqs. (19) and (20),

$$\begin{aligned} \delta x_0\left(t_j^+\right) &= \delta x_0\left(t_j^-\right) + \mathcal{P}_{jx}\left[x_0\left(t_j^-\right), u_0(t_j)\right]\delta x_0\left(t_j^-\right) \\ &\quad + \mathcal{P}_{ju}\left[x_0\left(t_j^-\right), u_0(t_j)\right]\delta u_0(t_j) \end{aligned} \tag{28}$$

$$\begin{aligned} \delta x_1\left(t_j^+\right) &= \delta x_1\left(t_j^-\right) + \mathcal{P}_{jx}\left[x_0\left(t_j^-\right), u_0(t_j)\right]\delta x_1\left(t_j^-\right) \\ &\quad + \mathcal{P}_{jxx}\left[x_0\left(t_j^-\right), u_0(t_j)\right]\delta x_0\left(t_j^-\right)x_1\left(t_j^-\right) \\ &\quad + \mathcal{P}_{jxu}\left[x_0\left(t_j^-\right), u_0(t_j)\right]\delta u_0(t_j)\,x_1\left(t_j^-\right) \\ &\quad + \mathcal{P}_{ju}\left[x_0\left(t_j^-\right), u_0(t_j)\right]\delta u_1(t_j) \\ &\quad + \mathcal{P}_{jux}\left[x_0\left(t_j^-\right), u_0(t_j)\right]\delta x_0\left(t_j^-\right)u_1(t_j) \\ &\quad + \mathcal{P}_{juu}\left[x_0\left(t_j^-\right), u_0(t_j)\right]\delta u_0(t_j)\,u_1(t_j) \\ &\quad + k\mathcal{P}_{jx}\left[x_0\left(t_j^-\right), u_0(t_j)\right]\delta x_0\left(t_j^-\right) \\ &\quad + k\mathcal{P}_{ju}\left[x_0\left(t_j^-\right), u_0(t_j)\right]\delta u_0(t_j) \end{aligned} \tag{29}$$

By substituting Eqs. (28), (29), and an expansion of λ into Eq. (27), grouping by powers of ϵ, and noting that Eq. (27) must be true for arbitrary $\delta x_0(t_j^-)$, $\delta x_1(t_j^-)$, $\delta u_0(t_j)$, and $\delta u_1(t_j)$, the following necessary conditions are obtained:

$$\lambda_0^T\left(t_j^+\right)\mathcal{P}_{ju}\left[x_0\left(t_j^-\right), u_0(t_j)\right] = 0 \tag{30}$$

$$-\lambda_0^T\left(t_j^-\right) + \lambda_0^T\left(t_j^+\right)\left\{I + \mathcal{P}_{jx}\left[x_0\left(t_j^-\right), u_0(t_j)\right]\right\} = 0 \tag{31}$$

$$\lambda_1^T\left(t_j^+\right)\mathcal{P}_{ju}\left[x_0\left(t_j^-\right), u_0(t_j)\right] + \lambda_0^T\left(t_j^+\right)\left\{\mathcal{P}_{jux}\left[x_0\left(t_j^-\right), u_0(t_j)\right] x_1\left(t_j^-\right) + \mathcal{P}_{juu}\left[x_0\left(t_j^-\right), u_0(t_j)\right] u_1(t_j) + k\mathcal{P}_{ju}\left[x_0\left(t_j^-\right), u_0(t_j)\right]\right\} = 0 \tag{32}$$

$$-\lambda_1^T\left(t_j^-\right) + \lambda_1^T\left(t_j^+\right)\left\{I + \mathcal{P}_{jx}\left[x_0\left(t_j^-\right), u_0(t_j)\right]\right\} + \lambda_0^T\left(t_j^+\right)\left\{\mathcal{P}_{jxx}\left[x_0\left(t_j^-\right), u_0(t_j)\right] x_1\left(t_j^-\right) + \mathcal{P}_{jxu}\left[x_0\left(t_j^-\right), u_0(t_j)\right] u_1(t_j) + k\mathcal{P}_{jx}\left[x_0\left(t_j^-\right), u_0(t_j)\right]\right\} = 0 \tag{33}$$

By combining Eqs. (30) and (31),

$$\lambda_0^T\left(t_j^-\right)\left\{I + \mathcal{P}_{jx}\left[x_0\left(t_j^-\right), u_0(t_j)\right]\right\}^{-1}\mathcal{P}_{ju}\left[x_0\left(t_j^-\right), u_0(t_j)\right] = 0 \tag{34}$$

which determines $u_0(t_j)$ implicitly. Then, Eq. (31) can be rewritten as

$$\lambda_0^T\left(t_j^+\right) = \lambda_0^T\left(t_j^-\right)\left\{I + \mathcal{P}_{jx}\left[x_0\left(t_j^-\right), u_0(t_j)\right]\right\}^{-1} \tag{35}$$

which determines $\lambda_0^T(t_j^+)$. Likewise, Eq. (33) can be rewritten as

$$\lambda_1^T\left(t_j^+\right) = \left(\lambda_1^T\left(t_j^-\right) - \lambda_0^T\left(t_j^+\right)\left\{\mathcal{P}_{jxx}\left[x_0\left(t_j^-\right), u_0(t_j)\right] x_1\left(t_j^-\right) + \mathcal{P}_{jxu}\left[x_0\left(t_j^-\right), u_0(t_j)\right] u_1(t_j) + k\mathcal{P}_{jx}\left[x_0\left(t_j^-\right), u_0(t_j)\right]\right\}\right) \times\left\{I + \mathcal{P}_{jx}\left[x_0\left(t_j^-\right), u_0(t_j)\right]\right\}^{-1} \tag{36}$$

which then can be substituted into Eq. (32) to obtain an expression implicit for $u_1(t_j)$. Once $u_1(t_j)$ is known, Eq. (36) can be used to determine $\lambda_1(t_j^+)$.

If the aerodynamic forces are small enough, a further simplification to Eqs. (30–36) is possible. For the zeroth-order terms, Eqs. (30) and (31) are approximated by

$$\lambda_0^T\left(t_j^-\right)\mathcal{P}_{ju}\left[x_0\left(t_j^-\right), u_0(t_j)\right] = 0 \tag{37}$$

$$\lambda_0^T\left(t_j^+\right) = \lambda_0^T\left(t_j^-\right) - \lambda_0^T\left(t_j^-\right)\mathcal{P}_{jx}\left[x_0\left(t_j^-\right), u_0(t_j)\right] \tag{38}$$

which are the same as Eqs. (30) and (31) except that some of the $\lambda_0(t_j^+)$ terms have been approximated by $\lambda_0(t_j^-)$. Equation (38) is recognized to be the first terms of a Taylor series expansion of Eq. (35), assuming small $\mathcal{P}_{jx}$, that is, assuming that the aerodynamics are relatively small. This has been found to be the case for certain problems. For the first-order terms, Eq. (33) is replaced by

$$\lambda_1^T\left(t_j^+\right) = \lambda_1^T\left(t_j^-\right) - \lambda_1^T\left(t_j^-\right)\mathcal{P}_{jx}\left[x_0\left(t_j^-\right), u_0(t_j)\right] \tag{39}$$

which is the same as Eq. (33) except that some terms involving $x_1(t_j^-)$ and $u_1(t_j)$ on the right-hand side have been neglected. Note that the form of Eqs. (38) and (39) also can be deduced directly from the second term of Eq. (25). These simplifications eliminate the need for iteratively solving for the quantities across the discontinuity.

The discontinuities in the zeroth-order states and costates allow for a better overall approximation to the optimal solution. At each discontinuity, the zeroth-order states and costates are adjusted by the approximate accumulated effects of the neglected dynamics. The discontinuities in the zeroth-order solution do not pose any practical problem. The guidance objective is to determine the control at the current time only; control in the future will be determined by repeating the guidance calculations with a new set of initial conditions. The utility of the approximation of the costates at the current time for determining the control is unaffected by discontinuities in the zeroth-order solution.

This approach to accounting for aerodynamic forces in the zeroth-order solution also allows for the following refinement for the interceptor problem. Rather than scaling the pulse function to the entire perturbing dynamics, as in Eq. (21), it is instead scaled to just the control-independent drag. This is physically reasonable because the angle of attack is small for most of the flight. This simplification eliminates some computations and increases the convergence of the zeroth-order problem, while still producing good zeroth-order solutions.

Finally, a simpler approach to including aerodynamic forces in the zeroth-order dynamics is possible for the coast phases. Because the zeroth-order equations do not include thrust terms, it is possible to introduce additional terms that are linear in the states into the zeroth-order problem and still retain an analytical solution. The form of these terms is justified physically; again they involve the portion of the drag not associated with angle of attack. Details of this approximation are provided in Sec. V.

V. Modified Equations of Motion for Coast Phases

For portions of flight during which there is no thrust, a different technique can be used to incorporate aerodynamic effects into the zeroth-order problem. The equations of motion during coast are Eqs. (1–4) with $T_{\rm net} = 0$. Now the quantity $\rho V C_{D_0}$ changes relatively slowly and can be approximated by a piecewise-constant function. Define

$$\bar{D}_0 = \left(\frac{\rho V S C_{D_0}}{2m}\right)_{\rm avg} \tag{40}$$

where the average is taken over an interval chosen such that $\rho V C_{D_0}$ is nearly constant. Equations (3) and (4), written in terms of the small parameter ϵ, become

$$\frac{dw_1}{dt} = -\bar{D}_0 w_1 + \epsilon\frac{r_s}{H_\rho}\left[-g_t\frac{X_1}{\sqrt{X_1^2 + X_3^2}} + \bar{D}_0 w_1 - \frac{\rho V S}{2m}(C_D\, w_1 + C_L\, w_3)\right] \tag{41}$$

$$\frac{dw_3}{dt} = -\bar{D}_0 w_3 - g_s + \epsilon\frac{r_s}{H_\rho}\left[g_s - g_t\frac{X_3}{\sqrt{X_1^2 + X_3^2}} + \bar{D}_0 w_3 - \frac{\rho V S}{2m}(C_D\, w_3 - C_L\, w_1)\right] \tag{42}$$

[Contrast these with Eqs. (8) and (9).]

The zeroth-order equations of motion then are Eqs. (1) and (2), and

$$\frac{dw_1}{dt} = -\bar{D}_0 w_1 \tag{43}$$

$$\frac{dw_3}{dt} = -\bar{D}_0 w_3 - g_s \tag{44}$$

where, for clarity, the subscript indicating zeroth-order quantities has been left out.

The zeroth-order state differential equations are linear and nonhomogeneous; by the method of undetermined coefficients,[18] their integrals are written as

$$X_1(t) = X_1(t_i) + \frac{w_1(t_i)}{\bar{D}_0}\{1 - \exp[-\bar{D}_0(t - t_i)]\} \tag{45}$$

$$X_3(t) = X_3(t_i) + \left[\frac{w_3(t_i)}{\bar{D}_0} + \frac{g_s}{\bar{D}_0^2}\right] \times\{1 - \exp[-\bar{D}_0(t - t_i)]\} - \frac{g_s}{\bar{D}_0}(t - t_i) \tag{46}$$

$$w_1(t) = w_1(t_i)\exp[-\bar{D}_0(t - t_i)] \tag{47}$$

$$w_3(t) = w_3(t_i)\exp[-\bar{D}_0(t - t_i)] - (g_s/\bar{D}_0)\{[1 - \exp[-\bar{D}_0(t - t_i)]\} \tag{48}$$

where t_i is the time at the beginning of the coast phase. Also by the method of undetermined coefficients, the zeroth-order costates are

$$\lambda_{X_1}(t) = \lambda_{X_1}(t_i) \tag{49}$$

$$\lambda_{X_3}(t) = \lambda_{X_1}(t_i) \tag{50}$$

$$\lambda_{w_1}(t) = \lambda_{w_1}(t_i)\exp[-\bar{D}_0(t - t_i)] + \frac{\lambda_{X_1}(t_i)}{\bar{D}_0}\{1 - \exp[-\bar{D}_0(t - t_i)]\} \tag{51}$$

$$\lambda_{w_3}(t) = \lambda_{w_3}(t_i)\exp[-\bar{D}_0(t - t_i)] + \frac{\lambda_{X_3}(t_i)}{\bar{D}_0}\{1 - \exp[-\bar{D}_0(t - t_i)]\} \tag{52}$$

The first-order costates are calculated in the standard way. The zeroth- and first-order costates are used in Eq. (17) to produce the approximation to the optimal control.

VI. Relation to Previous Work

The approach used to incorporate some of the effects of aerodynamics into the zeroth-order problem, described in Sec. IV, bears some resemblance to previous approaches. A description of those approaches and their relation to the current approach follows.

Feeley[3,4] noted that the analytical solution to the thrusting zeroth-order problem is preserved if the zeroth-order dynamics are augmented by constants or integrable functions of time only. He used piecewise-constant aerodynamic pulses to model the aerodynamic forces during the flight, which was powered throughout:

$$\frac{\mathrm{d}\boldsymbol{x}}{\mathrm{d}t} = \boldsymbol{f}(\boldsymbol{x}, \boldsymbol{u}) + \frac{\mathcal{P}_j}{m} + \epsilon\left[\boldsymbol{g}(\boldsymbol{x}, \boldsymbol{u}) - \frac{\mathcal{P}_j}{\epsilon m}\right] \tag{53}$$

The subscript j indicates the current interval; the number of intervals is chosen to give good performance. He selected the magnitudes of the pulses to account for the average state- and control-dependent forces in each interval along the vacuum zeroth-order trajectory:

$$\mathcal{P}_j = \frac{1}{t_{j+1} - t_j}\int_{t_j}^{t_{j+1}} \epsilon m \boldsymbol{g}(\boldsymbol{x}_{\text{vac}}, \boldsymbol{u}_{\text{vac}})\,\mathrm{d}t \tag{54}$$

He modeled mass as linear in time, so that the pulses integrated to logarithmic functions in the zeroth-order solution. Note that the pulses appear in the derivative equations and thus give rise to continuous integrals.

The Feeley approach has two drawbacks. First, the functional form of the zeroth-order costates is not changed; they are still continuous and either constant or linear functions of time, with a single slope for the entire flight. This can be a poor approximation to the actual costates, whose slope can vary significantly between endoatmospheric and exoatmospheric regions of flight (see Figs. 4 and 5 in Sec. VII). The functional form of the costates resulting from the approach described in Sec. IV, on the other hand, allows for a much better approximation to the optimal costates.

Second, the average aerodynamic forces are highly dependent on the angle-of-attack history, which can vary greatly between the vacuum and optimal trajectories. The latter problem can be addressed by solving the zeroth-order problem repeatedly, while reevaluating the pulse magnitudes each time along the latest zeroth-order trajectory. This is equivalent to simultaneously satisfying, while solving the zeroth-order problem, the set of equations

$$\mathcal{P}_j = \frac{1}{t_{j+1} - t_j}\int_{t_j}^{t_{j+1}} \epsilon m \boldsymbol{g}(\boldsymbol{x}_0, \boldsymbol{u}_0)\,\mathrm{d}t \tag{55}$$

Instead of $n + 1$ equations, solving the zeroth-order problem now involves solving $n(1 + N/2) + 1$ equations for $n(1 + N/2) + 1$ unknowns, where n is the number of states and N is the number of intervals chosen. The unknowns are the unknown states and costates at the initial time, the value of the final time, and the $nN/2$ pulse magnitudes.

Leung and Calise[11] suggested a generalization of this approach. Using the framework of the collocation method, they suggest writing the dynamics and Euler–Lagrange equations as

$$\frac{\mathrm{d}\boldsymbol{x}}{\mathrm{d}t} = \boldsymbol{f}(\boldsymbol{x}, \boldsymbol{u}) + \mathcal{P}_j + \epsilon\left[\boldsymbol{g}(\boldsymbol{x}, \boldsymbol{u}) - \frac{\mathcal{P}_j}{\epsilon}\right] \tag{56}$$

$$\frac{\mathrm{d}\boldsymbol{\lambda}}{\mathrm{d}t} = -\boldsymbol{f}_x^T(\boldsymbol{x}, \boldsymbol{u})\,\boldsymbol{\lambda} + \mathcal{Q}_j + \epsilon\left[-\boldsymbol{g}_x^T(\boldsymbol{x}, \boldsymbol{u})\,\boldsymbol{\lambda} - \frac{\mathcal{Q}_j}{\epsilon}\right] \tag{57}$$

where the pulses are evaluated at the midpoint of the interval along the zeroth-order trajectory:

$$\mathcal{P}_j = [\boldsymbol{f}(\boldsymbol{x}_0, \boldsymbol{u}_0) + \epsilon\,\boldsymbol{g}(\boldsymbol{x}_0, \boldsymbol{u}_0)]_{\text{mid}} \tag{58}$$

$$\mathcal{Q}_j = \left[-\boldsymbol{f}_x^T(\boldsymbol{x}_0, \boldsymbol{u}_0)\,\boldsymbol{\lambda}_0 - \epsilon\,\boldsymbol{g}_x^T(\boldsymbol{x}_0, \boldsymbol{u}_0)\,\boldsymbol{\lambda}_0\right]_{\text{mid}} \tag{59}$$

Leung and Calise found that the state pulse functions $\mathcal{P}_j$ are not necessary for heavy launch vehicle guidance and, further, that the zeroth-order costate equations can be simplified:

$$\frac{\mathrm{d}\boldsymbol{x}}{\mathrm{d}t} = \boldsymbol{f}(\boldsymbol{x}, \boldsymbol{u}) + \epsilon\,\boldsymbol{g}(\boldsymbol{x}, \boldsymbol{u}) \tag{60}$$

$$\frac{\mathrm{d}\boldsymbol{\lambda}}{\mathrm{d}t} = \mathcal{Q}_j + \epsilon\left[\frac{-\boldsymbol{f}_x^T(\boldsymbol{x}, \boldsymbol{u})\,\boldsymbol{\lambda}}{\epsilon} - \boldsymbol{g}_x^T(\boldsymbol{x}, \boldsymbol{u})\,\boldsymbol{\lambda} - \frac{\mathcal{Q}_j}{\epsilon}\right] \tag{61}$$

(Note that Leung and Calise wrote these equations in terms of a different parameter ϵ.) The number of equations that must be solved in the zeroth-order problem is $n(1 + N) + 1$.

The primary advantage to the Leung and Calise approach is that, with a judicious choice of intervals, the piecewise linear form of the zeroth-order costate equations can approximate well the optimal costates. The penalty, shared by the Feeley approach as well, is the increased number of equations to solve in the zeroth-order problem. Because the convergence of the solution to the zeroth-order problem is greatly dependent on the dimension of the problem, this is a significant disadvantage. Furthermore, for vehicles with long coast phases, the energy at thrust termination can be important in determining the shape of the coast arc. Therefore, the state pulse functions $\mathcal{P}_j$ may be required as well, raising the number of equations to $n(1+2N)+1$. On the other hand, the approach described in Sec. IV does not increase the number of simultaneous equations that must be solved in the zeroth-order problem; the number of equations remains $n + 1$. There is a computational burden associated with the evaluation of the discontinuities during the analytical integration of the zeroth-order equations, but no increase in the problem dimension.

VII. Results

The algorithm described here was used to generate approximate optimal intercept trajectories against moving targets. The results were compared to optimal trajectories generated using a numerical second-order sweep method.[12] The near-optimal guidance scheme also was compared to two other guidance schemes, a gravity turn followed by proportional navigation and a pure gravity turn.

The interceptor has a four-stage boost phase lasting 33 s, followed by an aerodynamically controlled coast to intercept. Neither a terminal propulsion system nor an explicit terminal guidance scheme was modeled; the results here are indicative of the early- and midcourse guidance performance with which a terminal system would have to contend. The target was modeled as moving along a ballistic re-entry path; the target motion was varied both spatially and temporally. Only a two-dimensional model was considered here, although application of the theory to three dimensions is straightforward.

Table 1 contains the intercept times for the optimal and approximate-optimal trajectories. For all trajectories, the miss distance (range at closest approach) was less than 1 m. For the longer-range interceptions, it is necessary to use pulse functions to include in the zeroth-order solution the effects of aerodynamics, as described in Secs. IV and V. Note that the intercept time for the approximate algorithm is very close to the optimal for the cases where an optimal trajectory is available. Note also the negligible miss for each target. Several of the interceptions are illustrated in Fig. 1.

The importance of including some aerodynamic forces in the zeroth-order solution is illustrated by Table 2. The table shows the zeroth- and first-order costates for the cases where the primary dynamics include no aerodynamics and where the primary dynamics include pulse aerodynamics. Without aerodynamics in the primary dynamics, the first-order corrections to the costates swamp the zeroth-order approximations, in violation of the assumption that the higher-order corrections are small compared to the zeroth-order quantities. The practical consequence is that, without aerodynamics

Table 1 Interceptions against various targets

	Intercept position, m		Intercept time, s	
Pulse	X_1	$X_3 - r_s$	Actual	Optimal
No	64,087	26,697	36.228	36.028
No	71,274	31,774	39.221	
No	92,329	45,825	48.033	
No	134,513	70,280	65.621	
No	176,981	89,926	83.056	
No	224,672	106,036	102.217	
No	281,132	94,853	120.777	120.766
No	307,857	87,364	130.856	
No	336,559	79,810	139.884	
Yes	445,630	37,792	179.046	178.712
Yes	476,970	29,725	190.911	
Yes	525,210	14,933	209.312	
Yes	545,374	7,512	217.014	
Yes	562,804	−2,403	223.566	

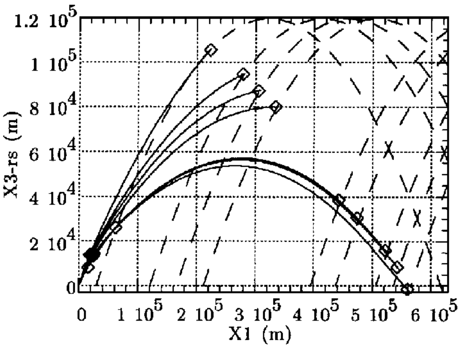

Fig. 1 Interceptions against various targets.

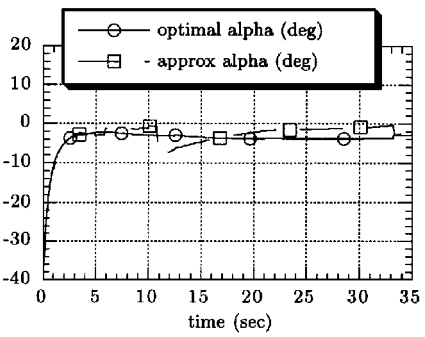

Fig. 2 Control during boost (179-s trajectory).

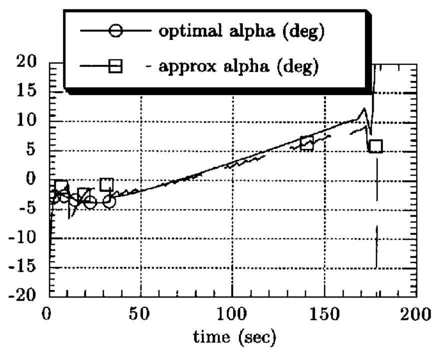

Fig. 3 Control (179-s trajectory).

in the primary dynamics, the control is poor and zeroth-order solution does not converge after about the second stage. On the other hand, the near-optimal guidance law that includes aerodynamics in the zeroth-order problem produces controls that are quite close to the optimal, as shown in Figs. 2 and 3.

More insight can be gained into the importance of the pulse aerodynamics by examining the zeroth-order costate trajectories (Figs. 4 and 5). The costates shown are not the result of a closed-loop

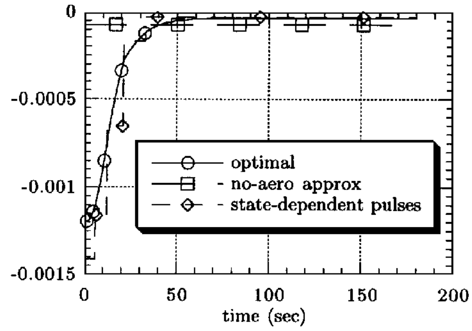

Fig. 4 Effect of pulses on X_3 zeroth-order Lagrange multipliers (179-s trajectory).

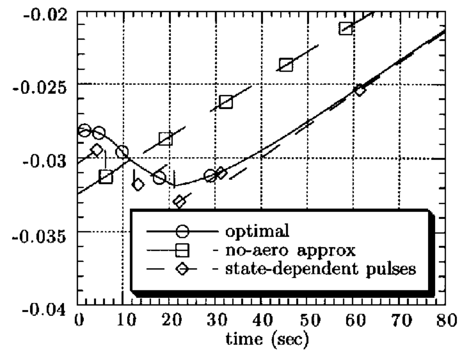

Fig. 5 Effect of pulses on w_1 zeroth-order Lagrange multipliers (179-s trajectory).

guidance law flown out to interception, but rather are the quantities predicted by the first guidance pass. With no aerodynamics in the primary dynamics, the zeroth-order costates are linear and cannot approximate the nonlinear, nonmonotonic optimal costates. With aerodynamic pulses in the primary dynamics, though, the zeroth-order costates are piecewise linear and can mimic the optimal costates well.

Finally, the near-optimal guidance law was compared with two simple guidance laws to get some idea of the relative performance. A gravity-turn guidance law was implemented by calculating the appropriate flight-path angle at the end of the pitchover maneuver and then flying a gravity turn (that is, a zero angle of attack) trajectory thereafter in an open-loop fashion. The flight-path angle at the end of the pitchover maneuver was calculated by iteratively integrating the full equations of motion until the predicted target miss was zero, within the resolution of the numerical integration. Another guidance law used this same algorithm until the final portion of the flight, when the guidance switched to proportional navigation.

The gravity turn and gravity turn plus proportional navigation give reasonable performance under nominal conditions. Their weakness, of course, is that they do not respond well to off-nominal conditions. To illustrate this, the three laws were compared for cases in which the actual thrust was either 100 or 101% of the value used in the guidance calculations. The comparison was done for the 179-s trajectory. The results are in Table 3. The approximate optimal guidance law provides better performance, as measured by the intercept time, miss due to guidance, and specific energy at intercept, especially under off-nominal conditions. In practice, the terminal phase would be powered and some terminal guidance law would be used to reduce the actual miss, including miss due to target state estimation error during boost. The miss tabulated here should be interpreted as indicative of the relative effort such a system would be required to expend to overcome boost guidance errors. The greater effort required for the simpler guidance schemes ultimately translates into greater weight and cost. Furthermore, the simpler guidance schemes fly less efficient trajectories, as indicated by the lower specific energies at intercept and by higher dynamic pressures. The peak dynamic pressure for the near-optimal guidance law is about 800 kPa, whereas it is about 1100 kPa for the gravity turn plus proportional navigation scheme.

Table 2 Costate estimates at time 0, with and without pulses

Case	λ_{X_1}	λ_{X_3}	λ_{w_1}	λ_{w_3}
No pulses, zeroth	$-1.9472596E-04$	$-7.5218748E-05$	$-3.2471950E-02$	$-1.2543266E-02$
No pulses, first	$-4.0318136E-05$	$-1.9412660E-03$	$3.4258386E-03$	$-1.6161806E-02$
No pulses, total	$-2.3504410E-04$	$-2.0164848E-03$	$-2.9046111E-02$	$-2.8705071E-02$
With pulses, zeroth	$-2.2001032E-04$	$-1.4148803E-03$	$-3.0583471E-02$	$-2.5026941E-02$
With pulses, first	$-8.7673496E-08$	$8.0784862E-05$	$1.4042609E-03$	$-2.0058933E-03$
With pulses, total	$-2.2009800E-04$	$-1.3340954E-03$	$-2.9179210E-02$	$-2.7032834E-02$
Optimal	$-2.1440427E-04$	$-1.1963102E-03$	$-2.8421884E-02$	$-2.6577802E-02$

Table 3 Guidance performance, nominal and off-nominal conditions (179-s trajectory)

	100% thrust			101% thrust		
Scheme	Time, s	Miss, m	Sp. energy, m^2/s^2	Time, s	Miss, m	Sp. energy, m^2/s^2
Optimal	178.712	0	$4.22E6$			
Approx optimal	179.074	$1.418E-4$	$4.18E6$	177.998	$5.003E-7$	$4.27E6$
Gravity turn/pronav	181.450	84.033	$3.88E6$	180.305	1386.279	$3.99E6$
Pure gravity turn	181.376	5.840	$3.95E6$	180.246	1518.488	$4.05E6$

VIII. Conclusions

The near-optimal guidance law produced using a perturbation procedure is effective for boost and coast interceptor guidance against a wide range of target motion. The control and the intercept times are close to optimal, and the miss is negligible. This algorithm is feasible for implementation in an onboard computer.

For longer ranges, the aerodynamics cannot be considered to be merely perturbing forces. The primary dynamics must be written such that some of the effects of the aerodynamics are included. If they are not, the resulting approximations to the optimal control are poor or the algorithm breaks down altogether. Introducing approximations to the aerodynamics using narrow pulse functions is an effective way to include the important aerodynamic effects without expanding the dimension of the zeroth-order problem.

Acknowledgments

This work was supported by the Charles Stark Draper Laboratory, Grant DL-H-454752, by Air Force Office of Scientific Research Grant F49620-94-1-0084, and by a TRW doctoral fellowship. The authors also gratefully acknowledge the work of John Bain, who provided the optimal trajectory against which the approximate trajectories were compared.

References

[1]Nayfeh, A., *Perturbation Methods*, Wiley, New York, 1973, Chaps. 1, 2, 4.

[2]Van Dyke, M., *Perturbation Methods in Fluid Mechanics*, Academic, New York, 1964, Chaps. 1, 5.

[3]Feeley, T. S., "Approximate Optimal Guidance for the Advanced Launch System," Ph.D. Thesis, Dept. of Aerospace Engineering and Engineering Mechanics, Univ. of Texas, Austin, TX, 1991.

[4]Feeley, T. S., and Speyer, J. L., "Techniques for Developing Approximate Optimal Advanced Launch System Guidance," *Journal of Guidance, Control, and Dynamics*, Vol. 17, No. 5, 1994, pp. 889–896.

[5]Mishne, D., and Speyer, J. L., "A Guidance Law for the Aeroassisted Plane Change Maneuver in the Presence of Atmospheric Uncertainties," *Proceedings of the 25th IEEE Conference on Decision and Control*, Inst. of Electrical and Electronics Engineers, Piscataway, NJ, 1986, pp. 677–682.

[6]Speyer, J. L., and Crues, E. Z., "Approximate Optimal Atmospheric Guidance Law for Aeroassisted Plane-Change Maneuvers," *Journal of Guidance, Control, and Dynamics*, Vol. 13, No. 5, 1990, pp. 792–802.

[7]Ilgen, M. R., Speyer, J. L., and Leondes, C. T., "Robust Approximate Optimal Guidance Strategies for Aeroassisted Plane Change Missions: A Game Theoretic Approach," *Control and Dynamic Systems: Advances in Theory and Applications*, edited by C. T. Leondes, Vol. 52; Integrated Technology Methods and Applications in Aerospace Systems Design, Harcourt Brace Jovanovich, San Diego, CA, 1992, pp. 229–289.

[8]Calise, A. J., and Melamed, N., "Optimal Guidance of Aeroassisted Transfer Vehicles Based on Matched Asymptotic Expansions," *Journal of Guidance, Control, and Dynamics*, Vol. 18, No. 4, 1995, pp. 709–717.

[9]Melamed, N., and Calise, A. J., "Evaluation of an Optimal Guidance Algorithm for Aero-Assisted Orbit Transfer," *Proceedings of the AIAA Guidance, Navigation, and Control Conference*, AIAA, Washington, DC, 1992, pp. 632–640.

[10]Calise, A. J., and Melamed, N., "Matched Asymptotic Expansion of the Hamilton–Jacobi–Bellman Equation for Aeroassisted Plane-Change Maneuvers," *Proceedings of the AIAA Guidance, Navigation, and Control Conference*, AIAA, Washington, DC, 1993, pp. 456–465.

[11]Leung, M. S. K., and Calise, A. J., "A Hybrid Approach to Near-Optimal Launch Vehicle Guidance," *Proceedings of the AIAA Guidance, Navigation, and Control Conference*, AIAA, Washington, DC, 1992, pp. 7–21.

[12]Bain, J. R., Dougherty, J. J., and Speyer, J. L., "Approximate Optimal Real-Time Intercept Guidance," TR, Univ. of California, Los Angeles, CA, June 1994.

[13]Dougherty, J. J., and Speyer, J. L., "Improved Approximations for Near-Optimal Interceptor Guidance," AIAA Paper 95-3324, 1995.

[14]Selby, S. M., *Standard Mathematical Tables*, 12th ed., Chemical Rubber Co., Cleveland, OH, 1972.

[15]Crues, E. Z., *Approximate Optimal Guidance Schemes for Atmospheric Orbital Maneuvering*, Ph.D. Thesis, Dept. of Aerospace Engineering and Engineering Mechanics, Univ. of Texas, Austin, TX, 1989.

[16]Dougherty, J. J., and Speyer, J. L., "An Approximate Optimal Ballistic Intercept Guidance Law," *Proceedings of the 33rd IEEE Conference on Decision and Control*, Inst. of Electrical and Electronics Engineers, Piscataway, NJ, 1994, pp. 3871–3876.

[17]Bryson, A. E., and Ho, Y. C., *Applied Optimal Control*, Hemisphere, Washington, DC, 1975, Chaps. 1–8.

[18]Rainville, E. D., and Bedient, P. E., *Elementary Differential Equations*, Macmillan, New York, 1981, Chap. 7.